

## GREEN SYNTHESIS, CHARACTERIZATION AND BIOLOGICAL EVALUATION OF ZINC NANOPARTICLES FROM FLOWER EXTRACT OF *BRASSICA OLERACEA ITALICA*

IBRAR KHAN<sup>1\*</sup>, MAMOONA JEHANZEB<sup>1</sup>, RAMEEN NADEEM<sup>1</sup>, AKHTAR NADHMAN<sup>2</sup>, SADIQ AZAM<sup>1</sup>, INAM ULLAH<sup>1</sup> AND FARHAN AHMAD<sup>3</sup>

<sup>1</sup>Centre of Biotechnology and Microbiology, University of Peshawar, Pakistan.

<sup>2</sup>Institute of Integrative Biosciences, CECOS University, Peshawar, Pakistan.

<sup>3</sup>Department of Biotechnology, Bacha Khan University, Charsadda, Pakistan.

\*Corresponding author's email: [ibrarkhan1984@uop.edu.pk](mailto:ibrarkhan1984@uop.edu.pk).

### Abstract

The current work focused on green synthesis of Zinc nanoparticles (ZnNPs) using the aqueous extract of *Brassica oleracea italica* inflorescence acting as a reducing agent. The characterization of ZnNPs was done by UV visible spectrophotometer for confirmation of the zinc nanoparticles formation. Other techniques were also done including SEM for morphology, XRD for crystalline structure, EDX for elemental analysis, FTIR for functional groups determination and TGA for mass analysis. Spherical shape nanoparticles were found with size ranging between 100-500nm by SEM analysis. From analysis of TGA it was elucidated that the compound is thermally sensitive to temperature as weight reduction was observed with rise in temperature. The ZnNPs showed low activity against *Shigella dysenteria*, while a good antifungal activity was found against *Paecilomyces fulvus* (70%). Positive results were achieved against blood groups O<sup>+</sup>, O<sup>-</sup>, AB<sup>-</sup> and B<sup>-</sup> while performing the haemagglutination activity. In phytotoxic activity, more damaged plants were observed at low concentration of ZnNPs. From the above study, it is concluded that the selected plant can be used for nanoparticles synthesis for achieving good antifungal, haemagglutination and phytotoxic effects.

**Key words:** Zinc nanoparticles, *Brassica oleracea italica*, Antibacterial, Antifungal, Haemagglutination, Phytotoxic.

### Introduction

The wonder of modern medicine is nano-materials, as nanoparticles have the capability to kill the pathogenic organisms. Nano-particles synthesis (10-100nm) have become a key field of research due to their potential application in wide areas of science and technology (Ali *et al.*, 2017a; Khan *et al.*, 2016; Kavitha *et al.*, 2017; Ahmad *et al.*, 2017; Ali *et al.*, 2017b; Ali *et al.*, 2017c; Kamal *et al.*, 2016a; Kamal *et al.*, 2016b). There are different ways for synthesis of nano-particles, the green synthesis of nano-particles gaining rapidly attention due to one step synthesis reaction, eco-friendly and less toxic chemicals. Metal oxide nanoparticles have found extensive applications in the field of medicine in the past decades. Metal oxide nanoparticles can act as a catalyst and may be helpful in reduction/ elimination of the toxic hazardous chemicals from the environment (Islam *et al.*, 2016; Haider *et al.*, 2018; Ali *et al.*, 2018a; Kamal *et al.*, 2016c; Ali *et al.*, 2018b; Kamal *et al.*, 2018; Khan *et al.*, 2019; Kamal, 2019). One of the key nanoparticles known for effective pharmacological activity are the Zinc oxide nanoparticles (Sungkaworn, 2008; Mirzaei & Darroudi, 2017).

Plant-mediated synthesis of ZnNPs has taken central role because of its eco-friendly nature, easy availability, extensive biomass and simple protocol than conventional methods of synthesis. The ZnNPs are peculiar due to their substantial use as anticonvulsant, antiplasmodial, antibacterial, antifungal, antioxidant and hypolipidemic (Raj, 2015). Apart from this, it has a variety of applications in biomedical field (Bogutskaya *et al.*, 2013). These nanoparticles can absorb ultraviolet radiations and protect humans from damaging radiations

of sun and hence are used in sunscreen creams (Kamal *et al.*, 2015). *Brassica oleracea* belongs to the family *Brassicaceae* also known as mustard family (McMurray, 1999). *Brassica var. oleracea italica* originated in Italy but is now grown almost all over the globe (Lim, 2012). The use of *B. oleracea* helps in reduction of cholesterol level and has anti-inflammatory and antioxidant properties (Rice, 1995; Kaur & Kapoor, 2002). This plant contains vitamin K and calcium and thus is also beneficial for bone health (Dosz, 2014). *Brassica oleracea* is also reported for its anticancer potentials due to the presence of organo sulphur compounds and protects against cardiovascular diseases (Finley, 2005; Vasanthi *et al.*, 2009). Sulforaphane prevents neurodegeneration, inflammation, neuronal loss and oxidative stress. *Brassica oleracea* sprout contains Sulforaphane making it a potential source for the treatment of Parkinson's and Alzheimer disease. This plant has been reported for its potential to reduce the impact of particulate pollution on allergic diseases and asthma. As the selected plant is a good source of flavonoids, it can reduce the risk of incident diabetes (Tarozzi, 2013; Heber, 2014). *Brassica oleracea* is among the common cruciferous vegetables possessing high levels important secondary metabolites including flavonoids. The pharmacokinetics of this plant explains that during metabolism a variety of products are produced including isothiocyanate (Nettleton, 2006).

### Materials and Methods

**Collection of plant and extraction:** *Brassica oleracea italica* inflorescence, identified by Dr. Lal Badshah, Department of Botany, University of Peshawar, was

collected from Peshawar, Khyber Pakhtunkhwa, Pakistan. The inflorescence was washed with tap water to remove any dust particles, dried under shade and grounded to powdered form. The aqueous extract was prepared by boiling 25g of powdered inflorescence in 500ml of distilled water for 30 minutes, cooled and filtered via filter paper (Whatman No 1).

**Synthesis of zinc nanoparticles:** The first step in the synthesis was the mixing of aqueous extract (10ml) in 90ml (1mM) of Zinc Sulphate ( $ZnSO_4$ ) solution. The mixture was then kept for 2 hours in a water bath with constant stirring and the formation of zinc nanoparticles was observed by change in color; from pale yellow to light brown. The reaction was stopped by centrifuging at 10000 RPM for 10 mins and then washed 3 times with distilled water and ethanol. Lastly, the nanoparticles solution was desiccated at room temperature in sterile Petri dishes (Awwad *et al.*, 2012).

### Characterization of Zinc nanoparticles

**UV-Vis spectrophotometer:** To confirm the formation of ZnNPs, double beam UV-Vis spectrophotometer (Shimadzu UV-1800) was used. The wavelength of 200–600 nm was set to observe the absorption spectra of the extract to confirm the presence of synthesized ZnNPs.

**Scanning electron microscope:** In distilled water, small quantity of powdered ZnNPs was exposed on a copper grid carbon and dried using hot air to form thin films which were then subjected to Scanning Electron Microscope (SEM JSM-5910 Japan) to get images at 5000, 10000, 20000, 30000 and 60000 × magnification.

**Fourier transform infrared spectroscopy:** The FTIR spectrum of synthesized ZnNPs was obtained by FTIR instrument. The scanning was done at resolution of  $4cm^{-1}$  from 4000-450  $cm^{-1}$  for 4 scans and the gained information was evaluated by IR solution software.

**Thermo-gravimetric and differential thermal analysis:** Shimadzu DTG-60/DTG-60A was used to determine chemical and physical properties of ZnNPs. Mass loss and gain of synthesized nanoparticles were analyzed by raising the temperature at  $10^{\circ}C/min$ .

**Energy dispersive x-ray analysis:** To evaluate the elemental composition of ZnNPs, EDX (INCA200) analysis was used. The synthesized ZnNPs were exposed on dual sided gummed carbon tape which was then placed over a stub made of aluminum (Al).

**X-ray diffraction measurements:** For analyzing the ZnNPs shape and size (JEOL Japan, JDX-3532) X-Ray Diffractometer was used. In respective solution, glass plate was dipped to develop a layer of ZnNPs. The intensity of diffractions was figured at  $0.02^{\circ}/min$  at  $2\theta$  angles from  $10^{\circ}$  to  $80^{\circ}$  at the 2s time. The conditions of measurement were as follows wavelength= $1.5418 \text{ \AA}$ , current= $30 \text{ mA}$ , voltage= $20-40 \text{ kV}$  in presence of Cu K $\alpha$  radiation (Awwad *et al.*, 2012).

### Biological activities

**Antibacterial activity:** Using well diffusion method antibacterial activity of synthesized ZnNPs was checked against *Lactobacillus bulgaricus*, *Pseudomonas aeruginosa*, *Staphylococcus aureus*, *Escherichia coli*, and *Shigella dysenteriae*. Both nutrient agar and broth media were prepared, autoclaved and incubated for a day at  $37^{\circ}C$  to check for sterility. A uniform bacterial lawn, on sterile nutrient agar plates, was made by using bacterial cultures in nutrient broth. Sterile borer (6mm) was used for making wells, then added with  $100\mu L$  of the test samples (3 mg/mL of DMSO) in it and incubated at  $37^{\circ}C$  for 24 hours. DMSO was used as a negative while Amoxicillin as a positive control for determining percent zone of inhibition (Ahmad *et al.*, 2009).

**Antifungal activity:** The antifungal activity was carried out against *Aspergillus niger*, *Rhizopus stolonifer*, *Paecilomyces fulvus* and *Fusarium solani*. By using DMSO, the stock solution was prepared from synthesized ZnNPs (24mg/mL). On SDA media, all the chosen fungus were refreshed. The test tubes were autoclaved after pouring 4mL of SDA media. When the temperature reached  $50^{\circ}C$ , the synthesized ZnNPs ( $67\mu L$ ) were introduced in test tubes. The test tubes were kept in slanted position followed by incubation for 24hr at  $37^{\circ}C$  to check for sterility. Inoculation of fungal strains was done in sterile test tubes and incubated at  $28\pm 1^{\circ}C$  for 7 days (Ahmad *et al.*, 2016).

**Phytotoxic assay:** The phytotoxic potential of synthesized ZnNPs was measured against *Lemna minor* following standard procedure (Ahmad *et al.*, 2010). In methanol, the synthesized ZnNPs stock solutions were prepared and 10, 100 and  $1000\mu L$  were introduced into labeled Petri plates. Healthy fifteen plants with E-media (20mL) were put into their specific Petri plates once the solvent was evaporated followed by incubation in a growth chamber for 7 days at  $28\pm 1^{\circ}C$ . To determine the phytotoxic potential of the sample the counting of damaged plants was carried out.

**Haemagglutination activity:** In 50mL of distilled water, 0.47g of  $Na_2HPO_4$  and 0.453g of  $K_2HPO_4$  were dissolved separately to prepare phosphate buffer in 7:3 ratio. From stock solution (1mg ZnNPs/ 1ml of DMSO), different dilutions were made; 1:2, 1:4, 1:8 and 1:16, for the experiments. Blood was taken from the healthy persons and centrifuge as to get RBC's. RBC suspension (2%) and each of the test sample (1mL) was thoroughly mixed and incubated at  $37^{\circ}C$  for 30 minutes. Formation of rough (positive) and smooth (negative) button were checked for determining the heamagglutination potential of the test sample (Ahmad *et al.*, 2010).

### Results and Discussion

**UV-visible spectroscopy:** Confirmation of the synthesized ZnNPs was carried out using wavelength from 200-600nm. A strong peak was observed at 300nm, having an absorbance value of 0.82 indicating the formation of ZnNPs (Fig. 1). One of the reported study demonstrated the formation of ZnONPs, showing an absorption peak at 325nm, from aqueous extract of *Camellia sinensis*, and is supporting our results (Senthilkumar & Sivakumar, 2014).

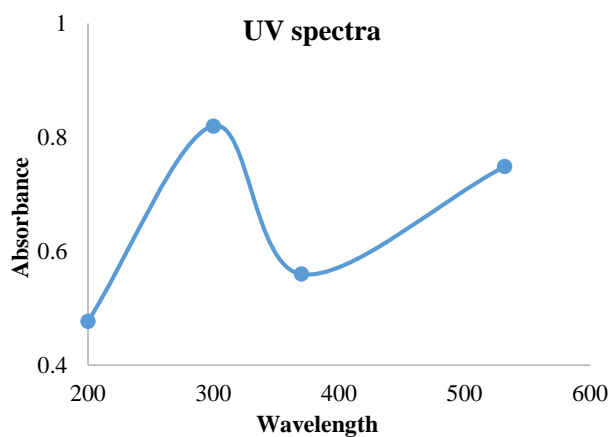


Fig. 1. UV Spectra of the synthesized ZnONPs.

**Scanning electron microscope:** Using different resolution power the size of particle ranged 96–136 nm as shown in (Fig. 2a, b, c). The surface morphology of ZnNPs was found nearly spherical. This was in agreement with the results of Raj *et al.*, 2015.

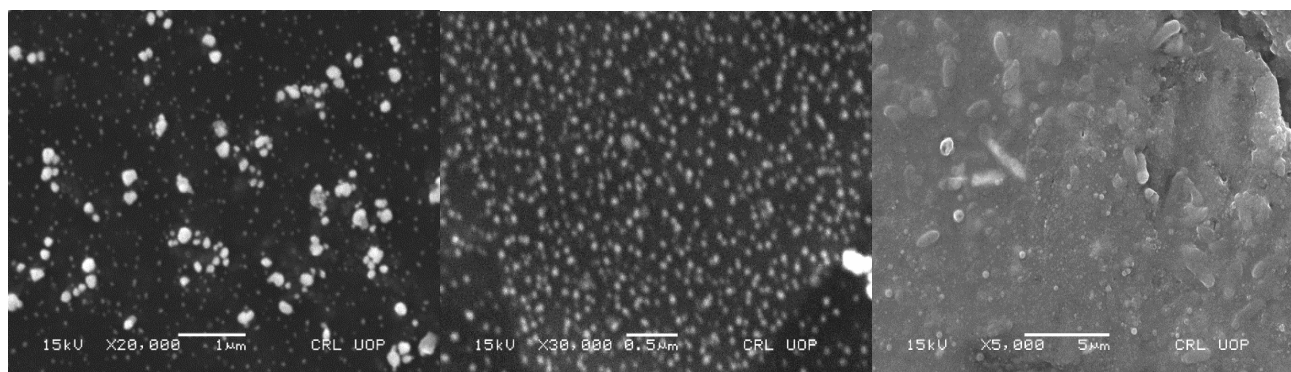


Fig. 2. SEM image of ZnNPs at 5000x, 20,000x and 30,000x.

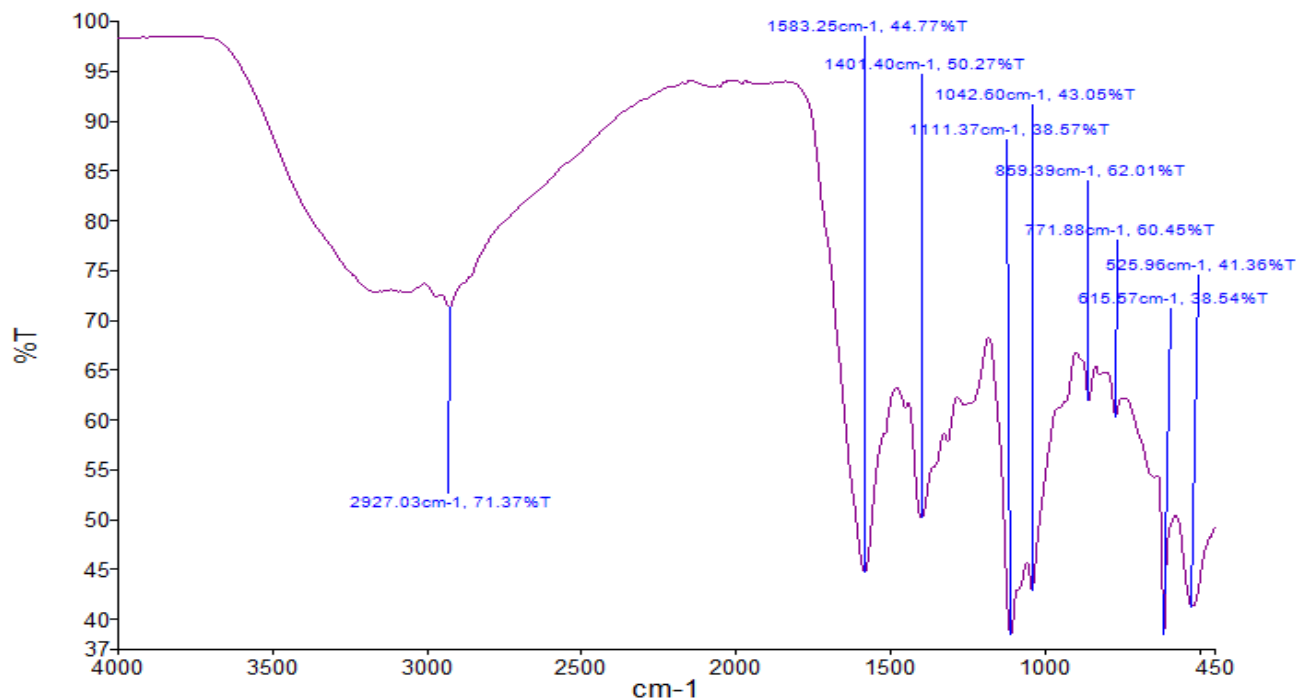


Fig. 3. FTIR analysis of synthesized ZnONPs.

**Fourier transform infrared spectroscopy:** The functional group analysis showed strong absorption peaks at 2927.03cm<sup>-1</sup> corresponding to C-H stretching vibrations of a carboxyl group, 1583.25cm<sup>-1</sup> for the presence of aromatic C=C bending, 1401.40cm<sup>-1</sup> and 1111.37cm<sup>-1</sup> showed C-H bending (Fig. 3). In previous study, the FTIR peaks of ZnNPs synthesized from *Andrographis paniculata* were at 1109cm<sup>-1</sup> and 2926cm<sup>-1</sup> showing C-O stretching vibration and C=O stretching of amides, respectively that were similar to our findings (Chen *et al.*, 2016).

**Thermogravimetric and differential thermal analysis:** The TGA curve in the (Fig. 4) shows weight reduction of 6.8, 5.9 and 4.6mg at 80°C, 210°C and 320°C. The significant weight reduction of 4-2.4mg occurred from 400-520°C which showed that the synthesized ZnNPs are thermally sensitive. In a previous reported study, weight reduction of synthesized ZnNPs was observed at 64-671°C range which was consistent with our results (Pathak *et al.*, 2013).

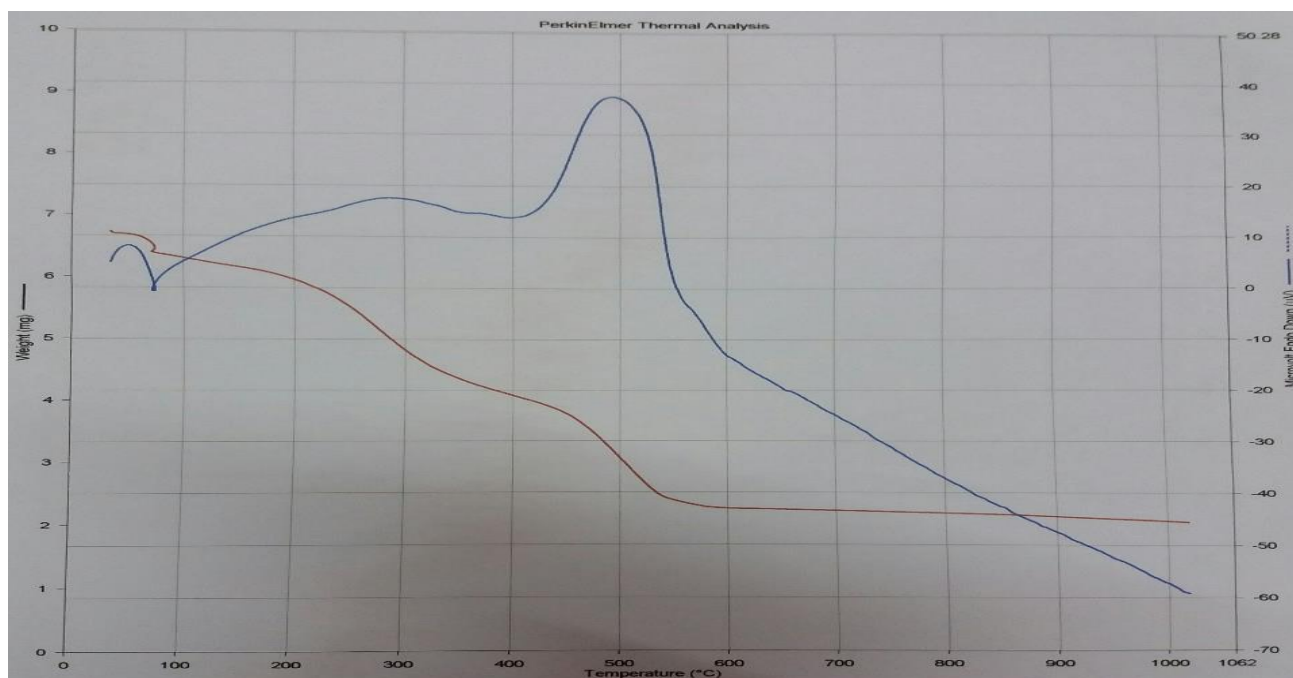


Fig. 4. TGA analysis of synthesized ZnONPs.

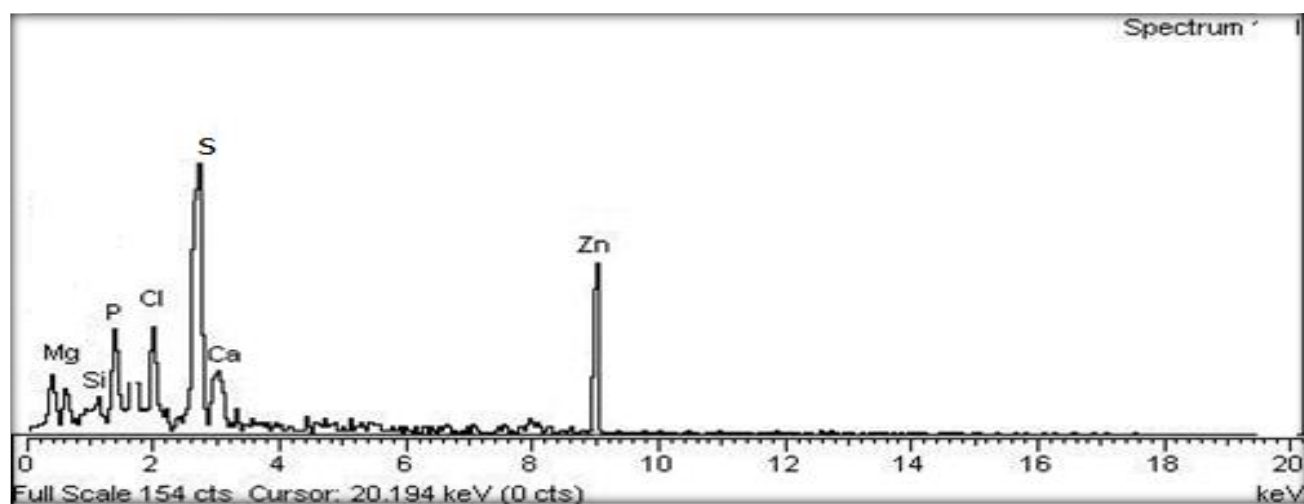


Fig. 5. EDX analysis of synthesized ZnNPs.

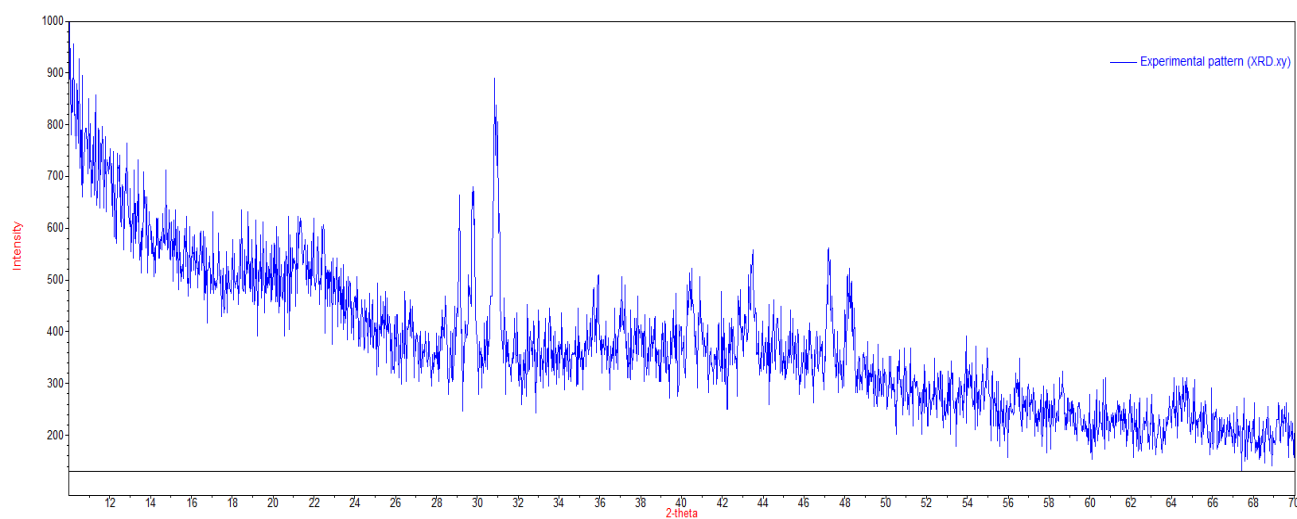


Fig. 6. XRD analysis of synthesized ZnNPs.

**Energy dispersive x-ray (EDX) analysis:** From EDX the elemental zinc gave a signal at 9kV with percent weight of 42.20% and atomic percentage of 45.23% (Fig. 5). The EDX profile showed presence of other elements such as Mg, Si, P, Cl and Si.

**X-ray diffraction:** From the XRD pattern, the strongest peaks were observed at around  $2\theta$  values of  $29^\circ$ ,  $30^\circ$ , and  $31^\circ$ . These values coincided with the reported literature (Rajendran & Sengodan, 2017). The determination of Bragg's reflection of ZnNPs by using XRD is useful because it showed peaks i.e. (111), (220) and (311) crystallographic planes that are characteristic of ZnONPs (Fig. 6).

**Antibacterial activity:** The ZnNPs showed antibacterial activity against *Shigella dysenteriae* with zone of inhibition of 11mm, while inactive against rest of the pathogens; *P. aeruginosa*, *E. coli*, *S. aureus* and *L. bulgaricus* (Table 1). In a reported study, the ZnNPs synthesized from *Trifolium pratense* flower extract showed antibacterial activity against *S. aureus*, *E. coli* and *P. aeruginosa* (Dobrucka & Długaszewska, 2016).

**Antifungal activity:** The ZnNPs showed good activity (70%) against *P. fulvus*, low activity against *A. niger* (35%) and no activity was observed against the remaining fungal pathogens (Table 2).

**Haemagglutination activity:** Positive results were presented against  $O^+$ ,  $O^-$ ,  $B^-$  and  $AB^-$  suggesting the presence of phytolectins in selected plant while negative results were observed for  $A^+$ ,  $A^-$ ,  $B^+$  and  $AB^+$  (Table 3). Our results are in line with another reported study where iron oxide nanoparticles showed hemagglutination at low concentration (Seabra and Duran, 2015).

**Phytotoxic assay:** The phytotoxic activity of ZnNPs was performed against *Lemna minor*. The ZnNPs showed good activity at a concentration of 10 and 100 while moderate activity was observed at a high concentration of 1000 $\mu$ l (Table 4). In reported studies, the growth inhibition was clearly observed with a reduction in numbers of fronds by treating the plant with AgNPs (Oukarroum, 2013; Gubbins *et al.*, 2011) and with ZnONPs.

**Table 1. Zone of inhibition of ZnNPs against the selected bacterial pathogens.**

S. No.	Name of bacteria	Inhibition zone diameter (mm)
1.	<i>Shigella dysenteriae</i>	11
2.	<i>Escherichia coli</i>	0
3.	<i>Pseudomonas aeruginosa</i>	0
4.	<i>Staphylococcus aureus</i>	0
5.	<i>Lactobacillus bulgaricus</i>	0

**Table 2. Antifungal activity of ZnNPs against selected fungal pathogens.**

S. No.	Name of fungus	Growth inhibition (%)
1.	<i>Paecilomyces fulvus</i>	70
2.	<i>Aspergillus niger</i>	35
3.	<i>Rhizopus stolonifer</i>	0
4.	<i>Fusarium solani</i>	0

**Table 3. Hemagglutination activity of ZnNPs against ABO blood groups.**

S. No	Blood group	1:2	1:4	1:8	1:16
1.	$O^+$	-	-	+	++
2.	$O^-$	+	+	-	-
3.	$A^+$	-	-	-	-
4.	$A^-$	-	-	-	-
5.	$B^+$	-	-	-	-
6.	$B^-$	++	+	-	-
7.	$AB^+$	-	-	-	-
8.	$AB^-$	+	+	-	-

+ = Rough button formation, - = Smooth button formation

**Table 4. Phytotoxic activity of ZnNPs against *L. minor*.**

S. No	Concentration ( $\mu$ l)	Total number of plants	Live	Dead
1.	10	15	4	11
2.	100	15	7	8
3.	1000	15	10	5

## Conclusion

The above study indicates that *Brassica Oleracea italica* can be used for the synthesis of ZnNPs. Synthesized ZnNPs have size range of 96-136nm with good antifungal activity against *paecilomyces fulvus* (70%), while low activity was observed against *Aspergillus niger* (35%). Antibacterial activity of the nano particles were checked and showed activity against *Shigella dysenteriae* with zone of inhibition of 11mm was observed. Positive results were presented against  $O^+$ ,  $O^-$ ,  $B^-$  and  $AB^-$  while negative results were observed for  $A^+$ ,  $A^-$ ,  $B^+$  and  $AB^+$ . The ZnNPs showed good activity at a concentration of 10 and 100 $\mu$ l while moderate activity was observed at a high concentration of 1000 $\mu$ l. This shows that ZnONPs possessed good antifungal, antibacterial properties that can be employed for different purposes in our daily life.

## References

- Ahmad, I., S.B. Khan, T. Kamal and A.M. Asiri. 2017. Visible light activated degradation of organic pollutants using zinc-iron selenide. *J. Mol. Liq.*, 229: 429-435.
- Ali, F., S.B. Khan, T. Kamal, K.A. Alamry and A.M. Asiri. 2018. Chitosan-titanium oxide fibers supported zero-valent nanoparticles: Highly efficient and easily retrievable catalyst for the removal of organic pollutants. *Sci. Rep.*, 8: 6260.
- Ali, N. Awais, T. Kamal, M.U. Islam, A. Khan, S.J. Shah and A. Zada. 2018. Chitosan-coated cotton cloth supported copper nanoparticles for toxic dye reduction. *Int. J. Biol. Macromol.*, 111: 832-838.
- Ali, F., S.B. Khan, T. Kamal, Y. Anwar, K.A. Alamry and A.M. Asiri. 2017a. Bactericidal and catalytic performance of green nanocomposite based-on chitosan/carbon black fiber supported monometallic and bimetallic nanoparticles. *Chemosphere.*, 188: 588-598.
- Ali, F., S.B. Khan, T. Kamal, K.A. Alamry, A.M. Asiri T.R.A. Sobahi. 2017b. Chitosan coated cotton cloth supported zero-valent nanoparticles: Simple but economically viable, efficient and easily retrievable catalysts. *Sci. Rep.*, 7: 16957.
- Ali, F., S.B. Khan, T. Kamal, Y. Anwar, K.A. Alamry and A.M. Asiri. 2017c. Anti-bacterial chitosan/zinc phthalocyanine fibers supported metallic and bimetallic nanoparticles for the removal of organic pollutants. *Carbohydr. Polym.*, 173: 676-689.

- Awad, A.M., N.M. Salem and A.O. Abdeen. 2012. Biosynthesis of silver nanoparticles using *Olea europaea* leaves extract and its antibacterial activity. *Nanosci Nanotechnol.*, 2: 164-170.
- Ahmad, B., N. Ali, S. Bashir, M.I. Choudhary, S. Azam and I. Khan. 2009. Parasitocidal, antifungal and antibacterial activities of *Onosma griffithii* Vatke. *Afr J Biotechnol.*, 8: 5084-5087.
- Ahmad, B., S. Farah., B. Shumaila., K. Ibrar and A. Sadiq. 2016. Green synthesis, characterization and biological evaluation of AgNPs using *Agave americana*, *Mentha spicata* and *Mangifera indica* aqueous leaves extract. *IET Nanobiotechnol.*, 10(5): 281-287.
- Ahmad, B., A. Sadiq B. Shumaila, K. Ibrar., A. Achyut and I. Muhammad. 2010. Anti-inflammatory and enzyme inhibitory activities of a crude extract and a pterocarpan isolated from the aerial parts of *Vitex agnus castus*. *Biotechnol. J.*, 5: 1207-1215.
- Bogutska, K., Y.P. Sklyarov and Y.I. Prylutsky. 2013. Zinc and zinc nanoparticles: biological role and application in biomedicine. *Ukrainica Bioorganica Acta.*, 1: 9-16.
- Chen, X., O. O'Halloran and M.A. Jansen. 2016. The toxicity of zinc oxide nanoparticles to *Lemna minor* (L.) is predominantly caused by dissolved Zn. *Aquat. Toxicol.*, 174: 46-53.
- Dobrucka, R. and J. Długaszewska. 2016. Biosynthesis and antibacterial activity of ZnO nanoparticles using *Trifolium pratense* flower extract. *Saudi J. Biol. Sci.*, 23: 517-523.
- Dosz, E. 2014. Improving the health benefits of broccoli through myrosinase maintenance. *University of Illinois at Urbana-Champaign*.
- Finley, J.W. 2005. Proposed criteria for assessing the efficacy of cancer reduction by plant foods enriched in carotenoids, glucosinolates, polyphenols and seleno compounds. *Ann. Bot.*, 95: 1075-1096.
- Gubbins, E.J., L.C. Batty and J.R. Lead. 2011. Phytotoxicity of silver nanoparticles to *Lemna minor* L. *Environ Pollut.*, 159: 1551-1559.
- Haider, A., S. Haider, I.K. Kang, A. Kumar, M.R. Kummara, T. Kamal and S.S. Han. 2018. A novel use of cellulose based filter paper containing silver nanoparticles for its potential application as wound dressing agent. *Int. J. Biol. Macromol.*, 108: 455-461.
- Heber, D. 2014. Sulforaphane-rich broccoli sprout extract attenuates nasal allergic response to diesel exhaust particles. *Food Func.*, 5: 35-41.
- Islam, M.U., M. Wajid-Ullah, S. Khan, T. Kamal, U.S. Islam, N. Shah and J.K. Park. 2016. Recent advancement in cellulose based nanocomposite for addressing environmental challenges. *Recent Pat. Nanotech.*, 10: 169-180.
- Kaur, C. and H.C. Kapoor. 2002. Anti-oxidant activity and total phenolic content of some Asian vegetables. *Int. J. Food Sci. Technol.*, 37: 153-161.
- Kamal, T., I. Ahmad, S.B. Khan and A.M. Asiri. 2016. 2018. Agar hydrogel supported metal nanoparticles catalyst for pollutants degradation in water. *Desalin Water Treat.*, 136: 290-298.
- Kamal, T., N. Ali, A.A. Naseem, S.B. Khan and A.M. Asiri. 2016a. Polymer nanocomposite membranes for antifouling nanofiltration. *Recent Pat Nanotech.*, 10: 189-201.
- Kamal, T., Y. Anwar, S.B. Khan, S.T.M. Chani and A.M. Asiri. 2016b. Dye adsorption and bactericidal properties of TiO<sub>2</sub>/chitosan coating layer. *Carbohydr. Polym.*, 148: 153-160.
- Kamal, T., S.B. Khan and A.M. Asiri. 2016. Nickel nanoparticles-chitosan composite coated cellulose filter paper: An efficient and easily recoverable dip-catalyst for pollutants degradation. *Environ. Pollut.*, 218: 625-633.
- Kamal, T. 2019. Aminophenols formation from nitrophenols using agar biopolymer hydrogel supported CuO nanoparticles catalyst. *Polym Test.*, 77: 105896.
- Kamal, T., M.U. Islam, S.B. Khan and A.M. Asiri. 2015. Adsorption and photocatalyst assisted dye removal and bactericidal performance of ZnO/chitosan coating layer. *Int. J. Biol. Macromol.*, 81: 584-590.
- Kavitha, T., S. Haider, T. Kamal and M.U. Islam. 2017. Thermal decomposition of metal complex precursor as route to the synthesis of Co<sub>3</sub>O<sub>4</sub> nanoparticles: Antibacterial activity and mechanism. *J. Alloys Compd.*, 704: 296-302.
- Khan, S.B., S.A. Khan, H.M. Marwani, E.M. Bakhsh, Y. Anwar, T. Kamal, A.M. Asiri and K. Akhtar. 2016. Anti-bacterial PES-cellulose composite spheres: Dual character toward extraction and catalytic reduction of nitrophenol. *RSC Adv.*, 6: 110077-110090.
- Khan, M.S.J., T. Kamal, F. Ali, A.M. Asiri and S.B. Khan. 2019. Chitosan-coated polyurethane sponge supported metal nanoparticles for catalytic reduction of organic pollutants. *Int. J. Biol. Macromol.*, 132: 772-783.
- Lim, T.K. 2012. Edible medicinal and non-medicinal plants. *Springer*. Vol. 1.
- Mirzaei, H. and M. Darroudi. 2017. Zinc oxide nanoparticles: biological synthesis and biomedical applications. *Ceram Int.*, 43: 907-914.
- McMurray, J. 1999. The origin, distribution and classification of cultivated broccoli varieties. *Ethnobot. Leaflets.*, 1999. 1: 6.
- Nettleton, J.A. 2006. Dietary flavonoids and flavonoid-rich foods are not associated with risk of type 2 diabetes in postmenopausal women. *J. Nutr.*, 136: 3039-3045.
- Oukarroum, A. 2013. Silver nanoparticle toxicity effect on growth and cellular viability of the aquatic plant *Lemna gibba*. *Environ Toxicol. Chem.*, 32: 902-907.
- Pathak, C., M. Mandal and V. Agarwala. 2013. Synthesis and characterization of zinc sulphide nanoparticles prepared by mechanochemical route. *Superlattices Microstruct.*, 58: 135-143.
- Rajendran, S.P. and K. Sengodan. 2017. Synthesis and characterization of zinc oxide and iron oxide nanoparticles using sesbania grandiflora leaf extract as reducing agent. *Int. J. Nanosci.*, 1-7.
- Raj, A., R.S. Lawrence, M. Jalees and K. Lawrence. 2015. Antibacterial activity of zinc oxide nanoparticles prepared from *Brassica oleracea* leaves extract. *Int. J. Adv. Res.*, 3 (11): 322-328.
- Rice-evans, C.A. 1995. The relative antioxidant activities of plant-derived polyphenolic flavonoids. *Free Radic Res.*, 22: 375-383.
- Sungkaworn, T. 2008. The effects of TiO<sub>2</sub> nanoparticles on tumor cell colonies: fractal dimension and morphological properties. *Int. J. Medical Health Biomed Bioeng Pharm Eng.*, 2: 20-7.
- Senthilkumar, S. and T. Sivakumar. 2014. Green tea (*Camellia sinensis*) mediated synthesis of zinc oxide (ZNO) nanoparticles and studies on their antimicrobial activities. *Int. J. Pharm Pharm Sci.*, 6: 461-465.
- Seabra, A.B. and N. Duran. 2015. Nanotoxicology of metal oxide nanoparticles. *Metals.*, 5: 934-975.
- Tarozzi, A. 2013. Sulforaphane as a potential protective phytochemical against neurodegenerative diseases. *Oxid. Med. Cell Longev.*, 1-10.
- Vasanthi, H.R. S. Mukherjee and D.K. Das. 2009. Potential health benefits of broccoli-a chemico-biological overview. *Mini Rev. Med. Chem.*, 9: 749-759.